



Sinking cities in Indonesia: ALOS PALSAR detects rapid subsidence due to groundwater and gas extraction

Estelle Chaussard ^{a,*}, Falk Amelung ^a, Hasanudin Abidin ^b, Sang-Hoon Hong ^c

^a School of Marine and Atmospheric Science, University of Miami, USA

^b Institute of Technology, Bandung (ITB), Indonesia

^c Korea Aerospace Research Institute (KARI), Republic of Korea

ARTICLE INFO

Article history:

Received 6 September 2012

Received in revised form 15 October 2012

Accepted 16 October 2012

Available online xxxx

Keywords:

Subsidence

Interferometric synthetic aperture radar

SBAS time-series

Indonesia

ABSTRACT

We use interferometric synthetic aperture radar (InSAR) time-series analysis of ALOS L-band SAR data to resolve land subsidence in western Indonesia with high spatial and temporal resolution. The data reveal significant subsidence in nine areas, including six major cities, at rates up to 22 cm/year. Land subsidence is detected near Lhokseumawe, in Medan, Jakarta, Bandung, Blanakan, Pekalongan, Bungbulang, Semarang, and in the Sidoarjo regency. The fastest subsidence occurs in highly populated coastal areas particularly vulnerable to flooding.

We correlate the observed subsidence with surface geology and land use. Despite the fact that subsidence is taking place in compressible deposits there is no clear correlation between subsidence and surface geology. In urban areas we find a correlation between rapid, patchy subsidence and industrial land use and elsewhere with agricultural land use. This suggests that the subsidence is primarily caused by ground water extraction for industrial and agricultural use, respectively. We also observe subsidence associated with exploitation of gas fields near Lhokseumawe and in the Sidoarjo regency. A continuation of these high rates of subsidence is likely to put much of the densely populated coastal areas below relative sea level within a few decades.

© 2012 Elsevier Inc. All rights reserved.

1. Introduction

Lowlands are often densely populated and land use represents a high economic value. The shallow subsurface in these areas frequently contains young, compressible deposits. These soft deposits are particularly vulnerable to subsidence caused by natural compaction or anthropogenic activities. While natural compaction is causing slow subsidence in numerous deltas, such as in the Mississippi and Po deltas at 5 and 2 mm/year, respectively (Teatini et al., 2011; Törnqvist et al., 2008), ground water extraction is causing rapid subsidence in urban areas, such as Mexico City and Las Vegas at rates of tens of cm/year (Bell et al., 2002; Cabral-Cano et al., 2008).

Subsidence, particularly in combination with sea level rise, heavy rains (such as monsoon), or storms, aggravates inundation risk from the major rivers and widens the coastal areas affected by storm surges and tidal inundation. The costs associated with subsidence are enormous, directly, because of damages to buildings and infrastructures, and indirectly given the increase in flood risk and the threat to human life. Examples of recent flooding events likely amplified by land subsidence include the flooding of New Orleans following Hurricane Katrina in 2005 (Dixon et al., 2006) and the flooding of Bangkok in 2011 (Chan et al., 2012).

Traditional measurements of land subsidence rely on GPS and leveling data. Although these methods provide precise measurements, they are time consuming, costly, and only supply data at a few locations. Mapping land subsidence over extensive areas with high precision can be achieved using InSAR. InSAR has facilitated the monitoring of land subsidence in many metropolitan areas, such as Las Vegas (Amelung et al., 1999; Burbey, 2002; Hoffmann et al., 2001), Mexico City (Osmanoglu et al., 2011), Paris (Fruneau & Sarti, 2000), Naples (Tesauro et al., 2000), Venice (Bock et al., 2012), Lisbon (Heleno et al., 2011), and Shanghai (Damoah-Afari et al., 2007).

In Indonesia, leveling and GPS observations have revealed that land subsidence is occurring in several cities (Abidin et al., 2010, 2011a, 2011b). However, because of the limitations of these methods, the spatial pattern of subsidence remains unknown and the processes causing the subsidence remain unclear. Here we define the rates and spatial pattern of land subsidence in western Indonesia using InSAR time-series analysis. Such a detailed mapping enables the identification of the processes responsible for the land subsidence, and is also a necessary first step in the development of hazard mitigation plans.

This paper is organized as follows. We first discuss the general potential for land subsidence in Indonesia (Section 1). For this we describe the typical causes of land subsidence, the surface geology, and the population distribution. After summarizing the data and methods used (Section 2), we present the InSAR-measured land subsidence and relate it to the surface geology and land use (Section 3), and

* Corresponding author. Tel.: +1 3056134448.

E-mail address: echaussard@rsmas.miami.edu (E. Chaussard).

compare our results with previous surveys (Section 4). We then discuss the causes of the observed subsidence (Section 5) and why subsidence is observed only in these specific locations (Section 6). Finally, we describe the consequences and implications of the observed subsidence (Section 7).

2. Potential for land subsidence in Indonesia

2.1. Overview of the causes of land subsidence and their characteristics

Land subsidence can be caused by natural and anthropogenic processes. Natural land subsidence results either from isostatic sediment loading and natural compaction of Holocene deposits or from tectonic and volcanic activities. Anthropogenic subsidence results from processes such as fluid withdrawal, solid withdrawal (tunnel construction or mining), changes in surface water drainage, and sediment loading (Raucoules et al., 2007; Yuill et al., 2009). Land subsidence resulting from each of these processes is characterized by specific rates and spatial patterns (summarized in Table 1). We define the spatial patterns as follows: large-scale: > 100 km², local: 10–100 km², and patchy: < 10 km².

Subsidence due to tectonic or volcanic activities occurs only in areas with active faults and volcanoes. Natural subsidence due to compaction of compressible Holocene deposits results from dewatering and increase of the overburden stress in unconsolidated sediments, or oxidation and shrinkage in organic deposits. Subsidence due to this process covers large areas, correlates with the surface geology, and is characterized by homogeneous rates rarely exceeding a few mm/year (Dixon et al., 2006; Meckel et al., 2006; Teatini et al., 2011). This type of subsidence is often taking place in deltas and coastal marshlands where compressible deposits are common (Teatini et al., 2011; Törnqvist et al., 2008).

On the other hand, anthropogenic subsidence is generally one order of magnitude faster than natural subsidence (Meckel, 2008) and results from intense land modifications in environments with compressible deposits. Subsidence due to fluid withdrawal such as groundwater, oil, or gas extraction can occur at high rates of up to tens of cm/year. The faster the fluid is extracted, the faster is the decline in the fluid level (water table or oil and gas levels) and the faster the subsidence (Bell et al., 2002; Osmanoglu et al., 2011). Its spatial pattern varies from patchy to large-scale, correlating with the land use (Feng et al., 2008). Solid withdrawal induces subsidence with characteristics similar to fluid withdrawal but results from mining and tunneling activities (Guéguen et al., 2009). Changes in surface water drainage, such as land reclamation, urbanization, and agricultural use (harvesting), create subsidence due to the same mechanisms as

subsidence by natural compaction. Subsidence due to this process is limited to the first twenty years or so after land modification because its typical rates of few cm/year, occurring on a local to large-scale pattern, decrease exponentially with time (Sestini, 1996). Finally, sediment loading (artificially, e.g. by construction of high-rise buildings, or naturally by addition of deposits) induces compaction of clays, resulting in land subsidence at rates up to 5 cm/year, also decreasing exponentially in time (Mazzotti et al., 2009; Yan & Gong, 2002).

2.2. Surface geology and population distribution of western Indonesia

As described above, in most cases land subsidence results from the progressive compaction of compressible deposits. Compressible deposits refer to unconsolidated sediments with high initial porosity and compressibility and/or high organic content (clays, silts, peats, loose sand). Compressible deposits correspond to surficial deposits, often found near the mouths of rivers and along the bays (alluvial, fan, lake, or residual deposits), and swamp or lagoon deposits. Decreasing pore-water pressure within the aquifer system produces an increase of effective stress and account for the compaction of compressible deposits. The pressure changes induce both elastic and inelastic compaction (Terzaghi, 1925). The elastic subsidence depends on the compressibility of the aquifer and can be recovered if the water level rises again. The inelastic subsidence is a result of the rearrangement of the pore structure under an effective stress greater than the preconsolidation stress, and results in an irreversible lowering of the surface (Helm, 1978).

The general distribution of compressible deposits in western Indonesia is shown by the black contour in Fig. 1 (Geological Map of Indonesia, 2008). Compressible deposits are present on the east coast, and locally along the west coast of Sumatra. In Java, compressible deposits characterize the north coast, the central part of the south coast, and a few locations inside the island. The remaining parts of the islands are constituted of volcanic and metamorphic rocks or limestone. These deposits are relatively incompressible because of their rigid matrix and are less likely to experience subsidence (except in the case of dissolution of limestone, responsible for sinkholes).

Indonesian municipal water supply serves on average only 25% of the population and 1% of the industrial needs, forcing the population and industries to rely on groundwater extraction as an alternate way to access water (Delinom, 2008; Schmidt et al., 1990). Thus, in densely populated areas extraction of groundwater likely occurs. Fig. 1 presents the population density of western Indonesia and reveals that most of the areas with over 250 persons per km² are located on the island of Java. We expect to observe subsidence in these densely populated

Table 1

Characteristics associated with each subsidence process potentially affecting Indonesian cities. Tectonic subsidence is unlikely to cause the observed subsidence because there are no mapped active faults coinciding with the boundaries of the described subsidence areas. Similarly, the observed subsidence is unlikely due to volcanic activity since no volcanoes are located in the subsiding areas. For the 5 remaining processes we compile the typical rates and spatial patterns, as well as correlations between subsidence and surface geology and subsidence and land use (Y = correlation, N = no correlation). The subsidence characteristics can be related to the observations made in the subsiding areas of Indonesia to isolate their causes (Table 2). Large-scale pattern refers to areas of over 100 km², local to 10–100 km², and patchy to 10 km² or less. Compressible deposits refer to surficial (alluvial, fan, lake, and residual deposits) and swamp deposits. They are unconsolidated deposits with a high initial porosity and compressibility and/or a high organic content (loose sand, clays, silts, and peat). As land use we distinguish forest, agricultural, residential, industrial, and mixed (residential and industrial) usage. Recently developed areas correspond to areas affected by changes in the past 20 years.

Subsidence process		Rates	Spatial pattern	Surface geology	Correlation with surface geol.	Land use	Correlation with land use
Natural	Holocene sed. compaction	<1 cm/year	Large	Compressible deposits	Y	All types	N
Anthropogenic	Fluid withdrawal	Up to tens of cm/year	Large to patchy	Compressible deposits	N	Indust., mixed, and agricult. (water, gas, oil extraction)	Y
	Solid withdrawal	Up to tens of cm/year	Local to patchy	All deposits	N	Industrial (mining) Y	
	Surface water drainage	<5 cm/year	Large to local	Compressible deposits	N	Indust., mixed, and agricult. (harvest or recently developed areas)	Y
Mixed	Sediment loading (settlement)	<5 cm/year	Large (sed. load) Patchy (buildings)	Compressible deposits	– Slow subs.: Y – Rapid: N	Industrial and mixed (recent massive buildings)	Y

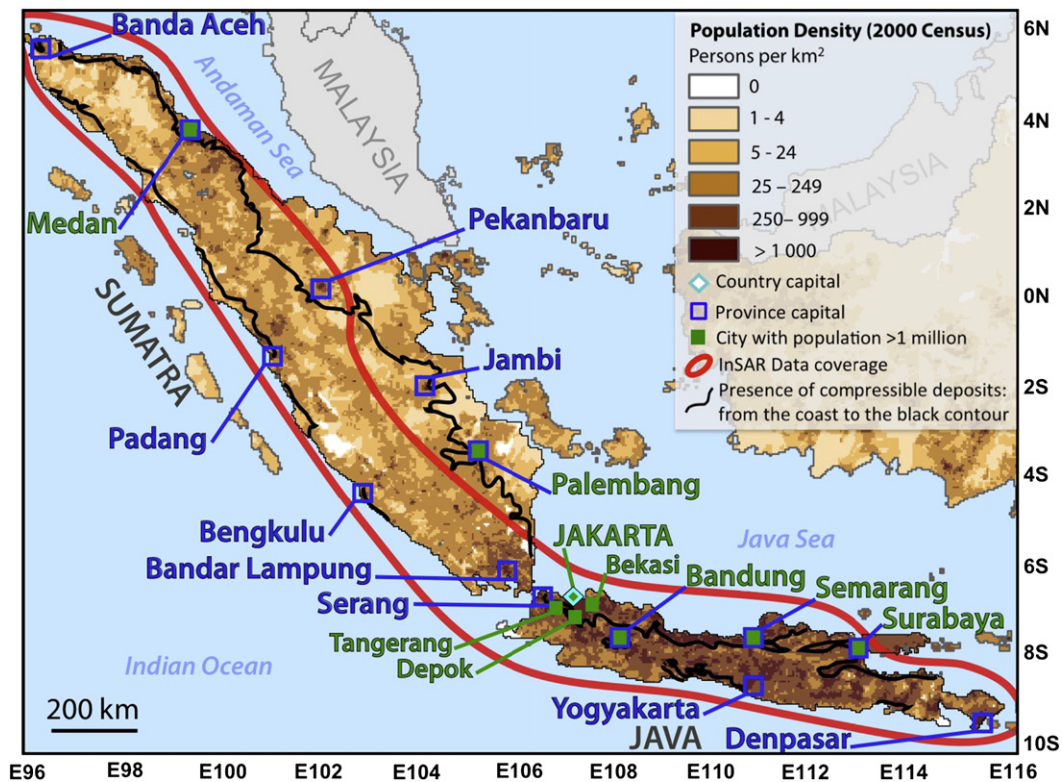


Fig. 1. Map of the population density in western Indonesia from the 2000 census. Cities with over 1 million inhabitants are marked by green squares; province capitals are shown with dark blue contoured squares. The distribution of compressible deposits is shown with the black line: the deposits are observed from the coast to the black contour or within the black contour. The area defined by the red line shows the InSAR ALOS data coverage available from the Alaska Satellite Facility. (For interpretation of the references to color in this figure legend, the reader is referred to the web version of this article.)

areas if they are located on compressible deposits. Cities such as Medan, Pekanbaru, Palembang, Jakarta, Depok, Bekasi, Bandung, Semarang, and Surabaya are likely to experience subsidence, as well as the populated coastal areas of Java outside city centers.

3. Data coverage and method

The red line in Fig. 1 shows our data coverage. We use over 900 SAR images from 33 ascending tracks acquired by the ALOS satellite between 2007 and 2009, to cover an area of 500,000 km² in Sumatra, Java and Bali. This coverage allows us to investigate 8 of the 9 major cities cited above (Palembang being left out) and to investigate subsidence over the entire island of Java. ALOS had a recurrent cycle of 46 days. For our 2 year period we used an average of 9 acquisitions per location.

L-band SAR images, such as PALSAR onboard ALOS, enable large-scale deformation mapping even in tropical areas, and provide for the first time consistent ground deformation data without spatial and temporal gaps (Chaussard & Amelung, in press). We perform a differential InSAR (D-InSAR) survey of western Indonesia by generating over 1300 interferograms. The D-InSAR technique measures ground displacement in the radar line-of-sight (LOS) by computing the phase difference of two temporally separated SAR images (Gabriel et al., 1989; Hanssen, 2001; Massonnet et al., 1993). After generation of the interferograms using the ROI_PAC software (Rosen et al., 2004), we use multiple SAR acquisitions of the same area to perform time-series analysis based on the small baseline subset (SBAS) method (Berardino et al., 2002). Interferograms with a maximum spatial baseline of 2600 m are phase-unwrapped and inverted for the phase with respect to the first acquisition. Coherence of each pixel is computed on the set of interferograms and we select only pixels with coherence above 0.7 to

eliminate bias from phase-unwrapping errors (Tizzani et al., 2007). Small baseline interferograms minimize the phase due to the DEM error in individual interferograms but not in the time-series, thus DEM error correction is necessary to remove the dependence of the displacement history to the perpendicular baseline history. We apply DEM error correction after the inversion of the network of interferograms following the technique developed by Fattahi and Amelung (in press). We do not use atmospheric filtering but we use pairwise logic to eliminate acquisitions with large atmospheric delays. We evaluate, based on the variance of the time dependent displacements, that the measurement noise for the entire survey is below ± 2 cm/year (green-yellow colors in Fig. 2) and varies depending on the number of SAR acquisitions and the atmospheric conditions. In the Indonesian cities the accuracy is likely better because of the lack of significant topography and associated atmospheric delays.

The limitation of this survey is that only ascending ALOS acquisitions are available, thus vertical and horizontal components of the deformation cannot be retrieved independently (Wright et al., 2004). However, previous GPS campaigns conducted in Jakarta, Bandung, and Semarang, showed that ground displacement is occurring principally vertically (Abidin et al., 2006, 2008; Lubis et al., 2011). Thus, we assume that the horizontal ground displacement is negligible and convert LOS into vertical displacement: $d_v = d_{LOS} / \cos\theta$; where d_v and d_{LOS} are the vertical and LOS displacement, respectively, and θ is the satellite incidence angle (we use 34.3° for ALOS). However, this assumption may not be appropriate near the edges of the subsiding areas. Vertical ground displacement is 21% more than LOS displacement, i.e., 1 cm of LOS displacement corresponds to 1.2 cm of vertical displacement. In most of this paper we use vertical subsidence rates converted from the observed LOS rates. When LOS is used it is explicitly stated.

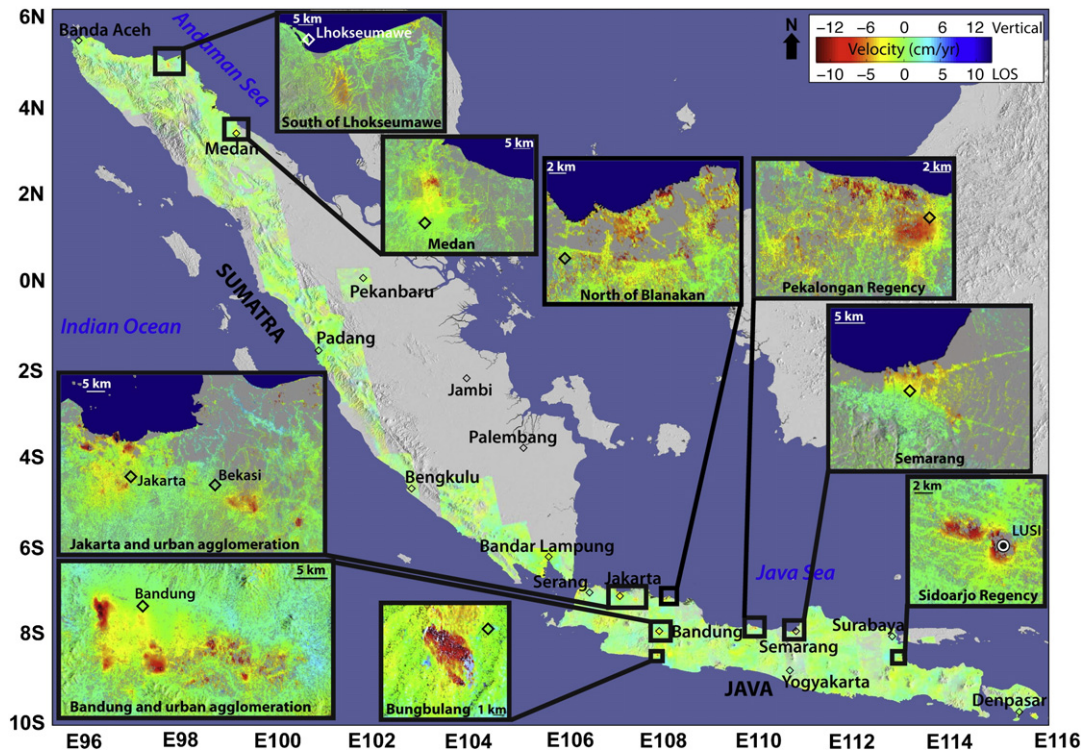


Fig. 2. Averaged 2006–2009 LOS velocity map of Sumatra, Java, and Bali, Indonesia, from ALOS InSAR time-series analysis, overlaying SRTM V4 DEM. Insets: zoom into the subsiding areas. The emplacement of major cities are shown by black diamonds and labeled for reference. The color scale shows red colors as negative LOS velocities (subsidence) and blue colors as positive LOS velocities (uplift). Vertical subsidence rates converted from the LOS rates are labeled on the color scale. (For interpretation of the references to color in this figure legend, the reader is referred to the web version of this article.)

4. Results: time-series reveal subsidence in nine locations

A map of the averaged LOS velocity identifies actively deforming areas (Fig. 2). Positive LOS velocities (blue colors) represent movement towards the satellite (e.g. uplift); negative LOS velocities (red colors) represent movement away from the satellite (e.g. subsidence). We detect land subsidence above the noise level in nine locations. In Sumatra we identify subsidence south of Lhokseumawe (population of 170,000) and in Medan (population of 2.1 million). In Java we detect subsidence in 4 urban areas: Jakarta, the capital and largest city of Indonesia (population of 9.5 million), Bandung (population of 2.4 million), Pekalongan (population of 200,000), and Semarang (population of 1.5 million). We additionally identify subsidence in 3 other locations of Java, outside major urban centers: near Blanakan (northeast Java), near Bungbulang (southeast Java), and in the Sidoarjo regency (East Java), affected by the eruption of the Lusi mud volcano since May 2006 (Mazzini et al., 2007).

4.1. Spatial pattern and rates of land subsidence

The land subsidence observations are summarized in Figs. 3–11. The figures are organized as follows: (a) shows the averaged velocity map and the surface geology, revealing the rates and spatial pattern of subsidence and the relation with the surface geology; (b) shows the vertical displacement time-series in locations with rapid subsidence (characterized by red to yellow colors in (a)); (c) shows the optical images of the locations experiencing rapid subsidence. Observations from these figures are summarized in Table 2.

We define the spatial patterns of land subsidence as follows: large-scale subsidence corresponds to subsidence with regular, homogeneous rates covering 100 km² or more; local subsidence covers 10–100 km²; and patchy subsidence covers less than 10 km². Average rates of subsidence of 4–6 cm/year (characterized by light blue to green colors in

Figs. 4–9 (a)) are observed at large-scales of 150, 450, 280, 150, 110, and 150 km² in Medan, Jakarta, Bandung, Blanakan, Pekalongan, and Semarang, respectively. In these locations, we find several areas of rapid subsidence (>6 cm/year, characterized by red to yellow colors) with a patchy distribution. They are located near the coast in Jakarta, Blanakan, Pekalongan, and Semarang.

Subsiding areas south of Lhokseumawe, near Bungbulang, and in the Sidoarjo regency are localized and cover 80, 15, and 25 km², respectively (Figs. 3, 10, and 11 (a)). We observe in these locations that the transition between areas with subsidence (red to yellow colors) and areas without subsidence (dark blue colors) occurs on a narrow zone (<1 km). This indicates that there is a sharp transition between the subsiding and the stable areas.

The time-series suggest nearly constant rates of subsidence in all the locations over the 2-year period spanned by the SAR acquisitions. The maximum vertical rates of subsidence observed are 11.3, 8.3, 21.8, 22.5, 12.0, 10.5, 13.0, 15.1, and 16.5 cm/year near Lhokseumawe, Medan, Jakarta, Bandung, Blanakan, Pekalongan, Semarang, Bungbulang, and in the Sidoarjo regency, respectively (Figs. 3 to 11 (b)).

4.2. Correlation between subsidence and surface geology

In Lhokseumawe, Jakarta, Bandung, Blanakan, Pekalongan, Semarang, and in the Sidoarjo regency, subsidence is taking place in surficial deposits (alluvial, fan, and lake deposits) (Figs. 3, 5–9, and 11 (a)). In Medan, subsidence is taking place both in surficial and swamp deposits (Fig. 4 (a)). In Semarang, we notice that the boundary between surficial deposits and limestone coincides with the southern limit of the subsiding area (Fig. 9 (a)). Near Bungbulang, subsidence is taking place in clastic and volcanic deposits (Fig. 10 (a)). Thus, in all the locations subsidence is taking place in compressible deposits (surficial and swamp deposits), except near Bungbulang. However, the subsidence rates do not correlate with the sediment type or thickness: multiple

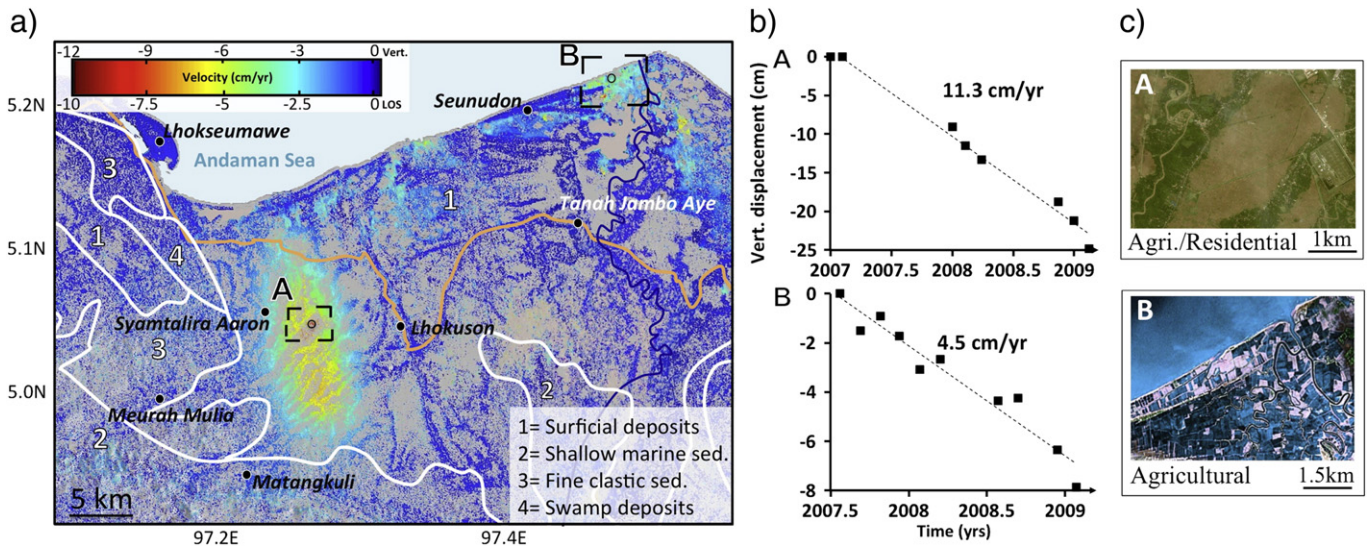


Fig. 3. Subsidence observed near Lhokseumawe. a) Average 2007–2009 velocity map. Roads are shown in light brown and main towns are labeled for reference. We correlate the subsidence distribution with the surface geology (combined bedrock and surficial geology and age data from the *Geological Map of Indonesia, 2008*). The contours of the geologic units are shown by white lines and referred to using white numbers. The black boxes show the locations of the Google Earth optical images displayed in c) corresponding to areas experiencing rapid subsidence. Black circles within the boxes show the location of the pixels whose time-series are showed in b). b) Vertical displacement time-series and corresponding linear rates of subsidence. c) Google Earth optical images showing the type of land use in rapidly subsiding areas. We distinguish forest, agricultural, residential, industrial, and mixed (residential and industrial) land use, based on the criteria described in the text. (For interpretation of the references to color in this figure legend, the reader is referred to the web version of this article.)

subsidence rates are observed in a single sediment unit and a given subsidence rate can be observed in different sediment units. This suggests that there is no clear correlation between subsidence and surface geology. Compressible deposits may be necessary, but other parameters also control the spatial distribution of subsidence.

4.3. Correlation between subsidence and land use

We test whether areas experiencing rapid, patchy subsidence (>6 cm/year, red to yellow colors) correlate with areas of intense groundwater extraction. We cannot use reported groundwater extraction volumes because of the large number of unregistered wells. Illegal extraction is believed to be as much as 120% of the registered extraction (Soetrisno, 1996). Groundwater extraction is categorized

in 2 types: shallow-water extraction for domestic use, and deep-water extraction at high rates for industrial and agricultural uses (Braadbaart & Braadbaart, 1997). Thus, we utilize land use as a proxy for the expected amount of groundwater extraction.

We use optical Google Earth imagery from 2006 to 2009 to classify the land use. We distinguish forest, agricultural, residential, industrial, and mixed (residential and industrial) land use. Green colors indicate forests and agricultural land use. Geometric patterns also indicate agricultural land use. Small habitations and red or brown colors indicate residential land use. Large buildings with white or gray roofs indicate industrial land use.

We notice, in six of the nine subsiding areas, a correlation between rapid, patchy subsidence and land use (Figs. 3–11 (c)). In Medan, Jakarta, Bandung, and Semarang rapid, patchy subsidence is occurring

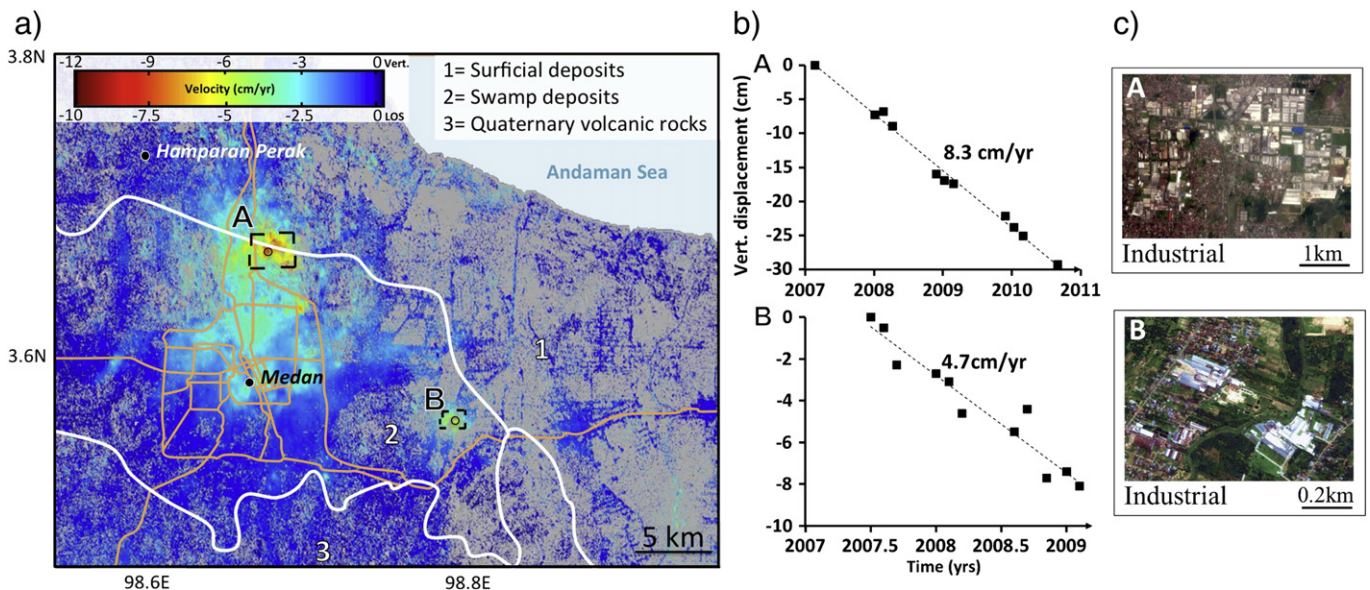


Fig. 4. Same as Fig. 3 for Medan. (For interpretation of the references to color in this figure legend, the reader is referred to the web version of this article.)

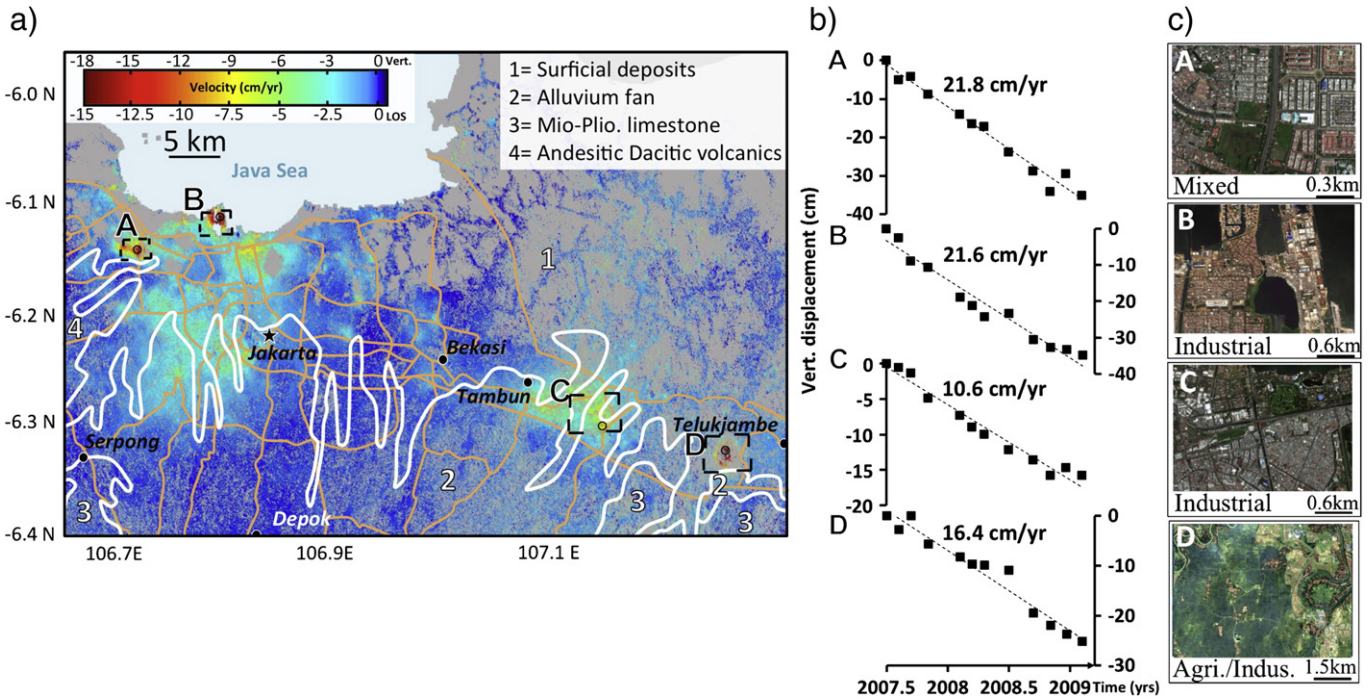


Fig. 5. Same as Fig. 3 for Jakarta. (For interpretation of the references to color in this figure legend, the reader is referred to the web version of this article.)

in industrial areas (Figs. 4 to 6 and 9 (c)), while on the coast north of Blanakan and around Pekalongan it correlates with agricultural areas (Figs. 7 and 8 (c)). In the remaining 3 locations, where subsidence areas have sharp transitions with the surrounding stable areas, the pattern of the subsidence does not correlate with the land use. South of Lhokseumawe and in the west of the Sidoarjo regency, subsidence is taking place in agricultural and residential areas (Figs. 3 and 11 (c)) and near Bungbulang subsidence is taking place in forests and agricultural areas (Fig. 10 (c)).

5. Comparison between InSAR and GPS

GPS surveys have been conducted in three Indonesian cities: Jakarta (Abidin et al., 2001, 2004, 2008, 2011a), Bandung (Abidin et al., 2011b), and Semarang (Abidin et al., 2010, 2012). GPS subsidence rates overlapping InSAR velocity maps are shown in the Supplementary material. In Jakarta, GPS campaigns between 1997 and 2005 show that the fastest subsidence is occurring near the coast at rates up to 15–25 cm/year. In Bandung GPS surveys between 2000 and

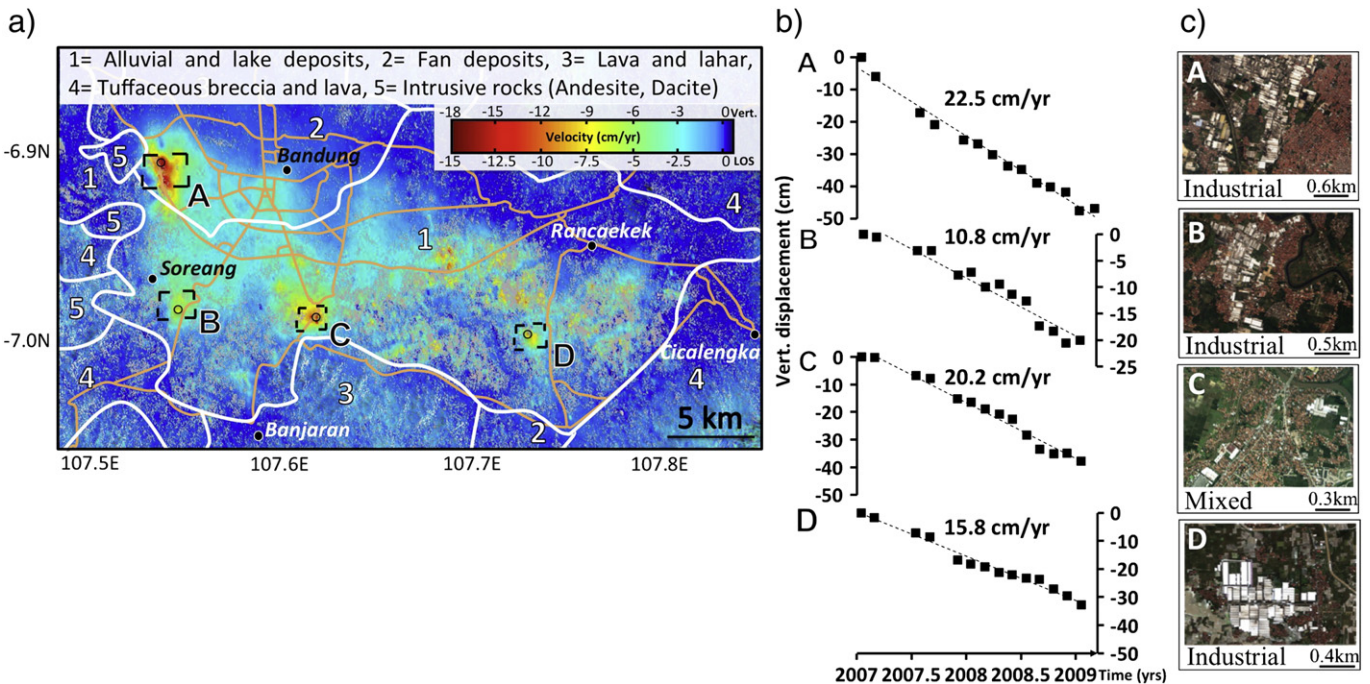


Fig. 6. Same as Fig. 3 for Bandung. (For interpretation of the references to color in this figure legend, the reader is referred to the web version of this article.)

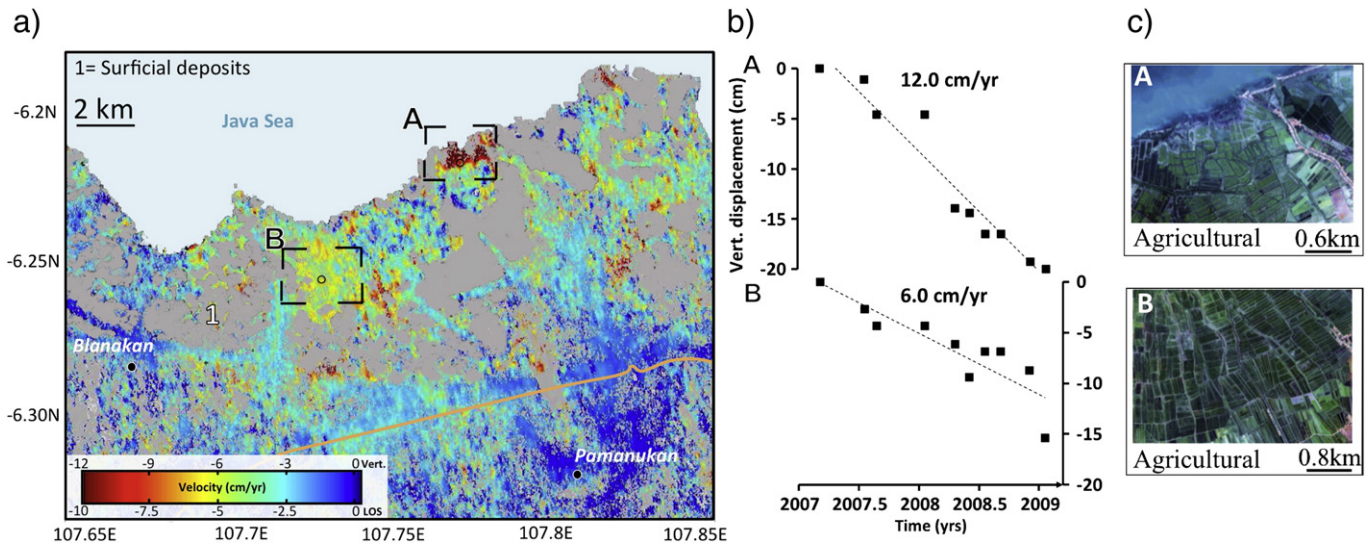


Fig. 7. Same as Fig. 3 for Blanakan. (For interpretation of the references to color in this figure legend, the reader is referred to the web version of this article.)

2010 show subsidence rates of 8–23 cm/year, the fastest subsidence occurring in the northwest of the city. In these two cities we observe a good agreement between GPS and InSAR observations both in rates and spatial distribution (Supplementary material Figs. S1 and S2, respectively). In Semarang, GPS surveys between 2008 and 2009 show a maximum subsidence of 13.5 cm/year along the coast, in agreement with our results. However, local differences between GPS and InSAR occur (Supplementary material Fig. S3), reflecting the fact that the subsidence rates are not constant or that local site effects affect GPS measurements. A subsidence map of Semarang derived from 2002 to 2006 PS-InSAR data is compared to our InSAR survey (Kuehn et al., 2010, Supplementary material Fig. S4). Even though the time spans do not overlap, the agreement is very good, suggesting that the difference between InSAR and GPS is due to local site effects.

6. Causes of subsidence in Indonesia

In Indonesia, subsidence is taking place at average rates of 4–6 cm/year over large-scales (light blue to yellow colors), while rapid subsidence (>6 cm/year, yellow to red colors) has a patchy distribution. We focus on identifying the causes of the latter using a qualitative approach. Quantitative modeling could help to better constrain the subsidence processes but this is beyond the scope of this

paper. It would require detailed information on the sediment properties (sediment thickness, porosity and permeability), water table and gas extraction rates, all of which is not readily available in Indonesia.

6.1. Urban areas: subsidence due to groundwater extraction for industrial use

Rapid, patchy subsidence in Medan, Jakarta, Bandung, and Semarang correlates with industrial land use (Figs. 4–6, 9). This suggests that groundwater extraction for industrial use is the main cause of the rapid land subsidence in these four cities.

We observe constant subsidence rates without any clear seasonal variability. There are two possible explanations for this. First, water could be extracted from confined aquifers that are little affected by seasonal recharge. Second, water extraction could occur at higher rates during the rainy season, compensating the recharge of the shallow, unconfined aquifers. Since stress changes are lower in unconfined aquifers it is improbable that any substantial subsidence would result from compaction occurring in unconfined units. Thus, it is very likely that the lack of seasonal variability reflects water extraction from confined aquifers. Since only deep wells are reaching confined aquifers (Braadbaart & Braadbaart, 1997), the lack of seasonal variability supports

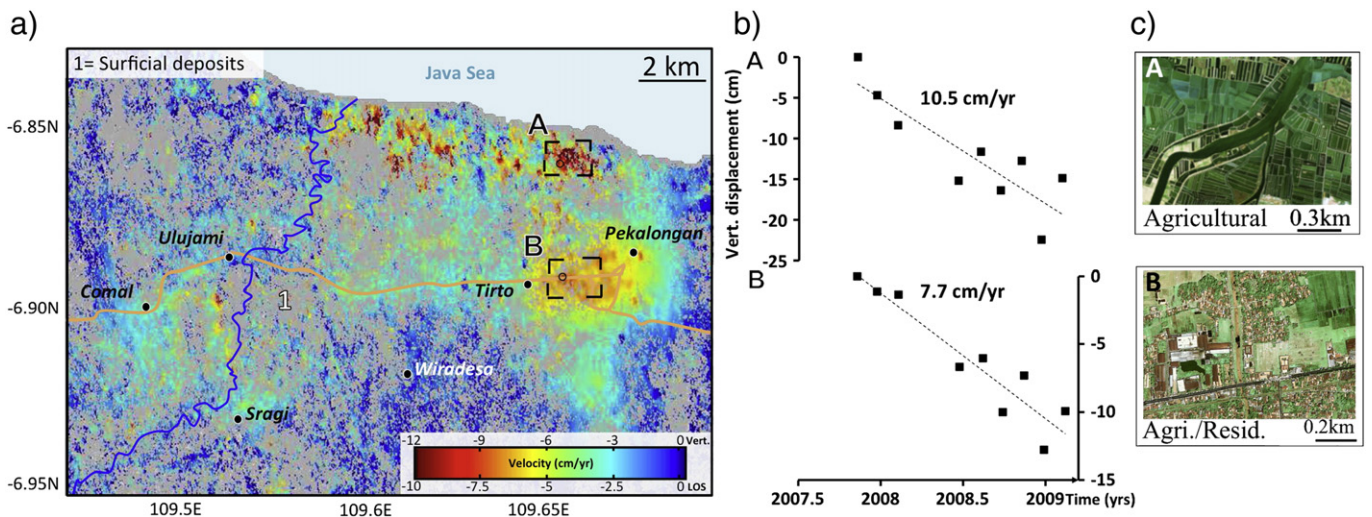


Fig. 8. Same as Fig. 3 for Pekalongan. (For interpretation of the references to color in this figure legend, the reader is referred to the web version of this article.)

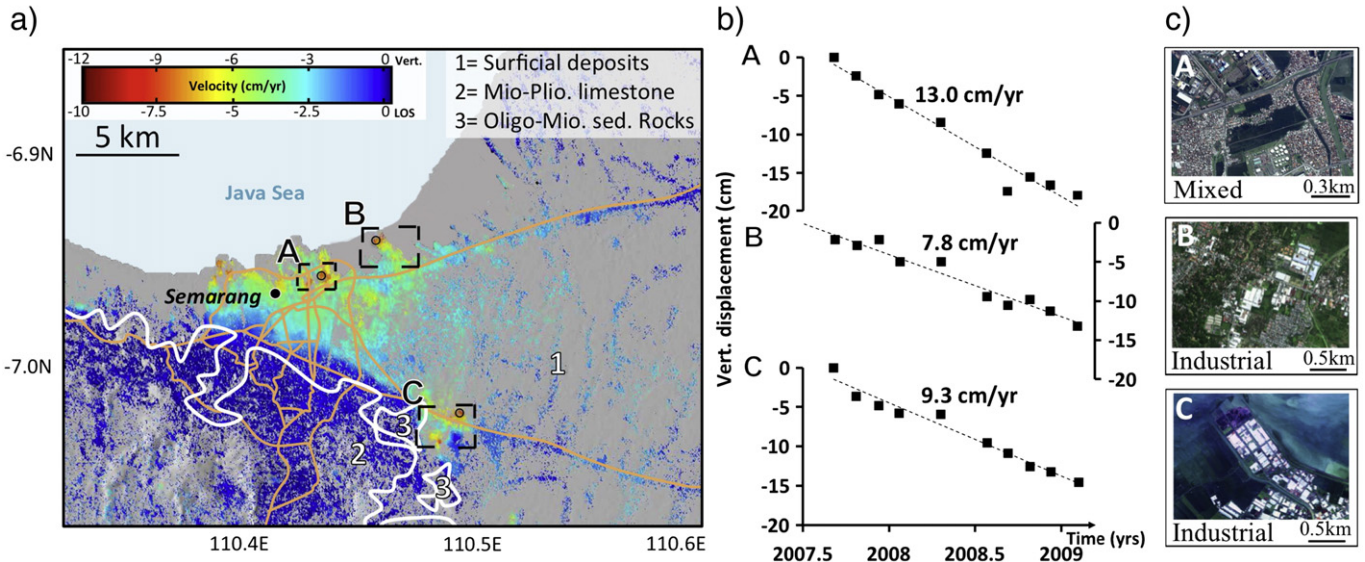


Fig. 9. Same as Fig. 3 for Semarang. (For interpretation of the references to color in this figure legend, the reader is referred to the web version of this article.)

that in Medan, Jakarta, Bandung, and Semarang industrial groundwater extraction is responsible for the rapid subsidence.

6.2. *Blanakan and Pekalongan: subsidence mainly due to groundwater extraction for agricultural use*

Rapid, patchy subsidence near Blanakan and Pekalongan varies from one field to the other, lacks significant seasonal variability, and correlates with agricultural land use (Figs. 7–8). These observations suggest that groundwater extraction for agricultural use is likely the main cause of rapid land subsidence and that some farmers extract more intensely groundwater than others. In these two cities we note a larger variance of the time dependent displacement than at the other locations (especially near Pekalongan) (Figs. 7–8 (b)). This variability may be due to differences in groundwater extraction rates owing to harvesting schedules or seasonality, and suggests that oxidation and shrinkage of organic deposits may contribute to the subsidence.

Atmospheric phase delay and backscattering effects can also be responsible for some of this variability.

6.3. *Lhokseumawe and Sidoarjo: subsidence due to gas extraction*

The subsidence bowl near Lhokseumawe is elongated north–south and covers 80 km² (Fig. 3). Its particular shape, the lack of direct correlation with land use, and its sharp transition with the stable surrounding areas make it unlikely to result from groundwater extraction. Interestingly, this subsidence area coincides with the Arun gas field. Gas is extracted from Lower and Middle Miocene reef deposits of ~300 m thickness and located over 3 km deep (Soeparjadi, 1983). We suggest that gas extraction causes the observed subsidence.

In the Sidoarjo regency, subsidence is taking place at 2 different locations: around Lusi mud volcano (Fig. 11, inset B) and west of Lusi, on an east–west 3 km-long area located in residential and agricultural areas (Fig. 11, inset A). The subsidence west of Lusi is located on the

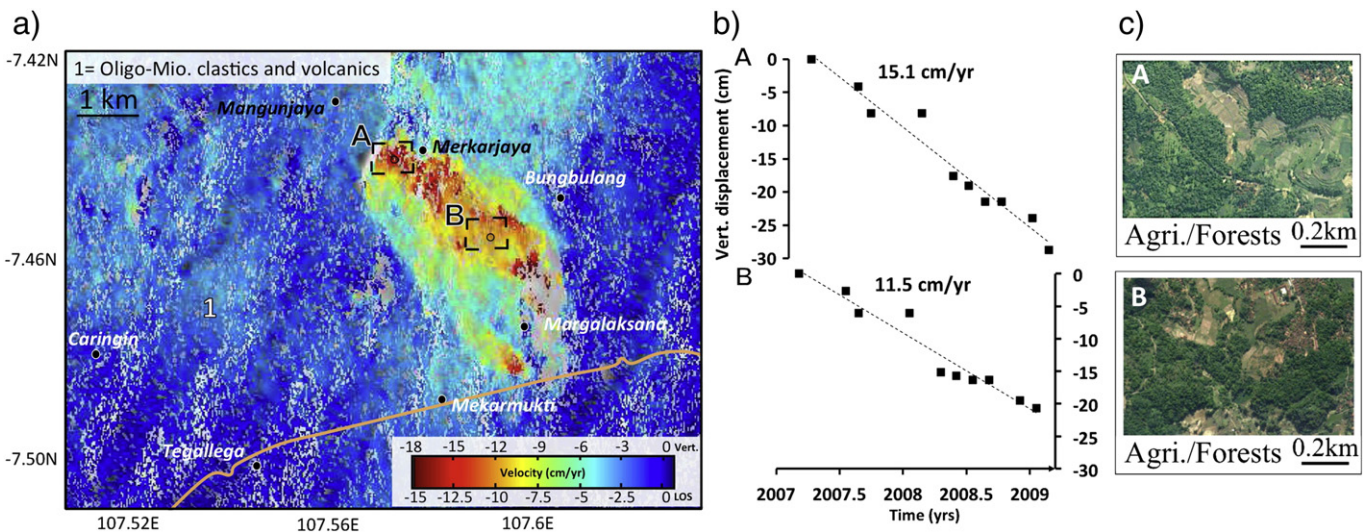


Fig. 10. Same as Fig. 3 for Bungbulang. (For interpretation of the references to color in this figure legend, the reader is referred to the web version of this article.)

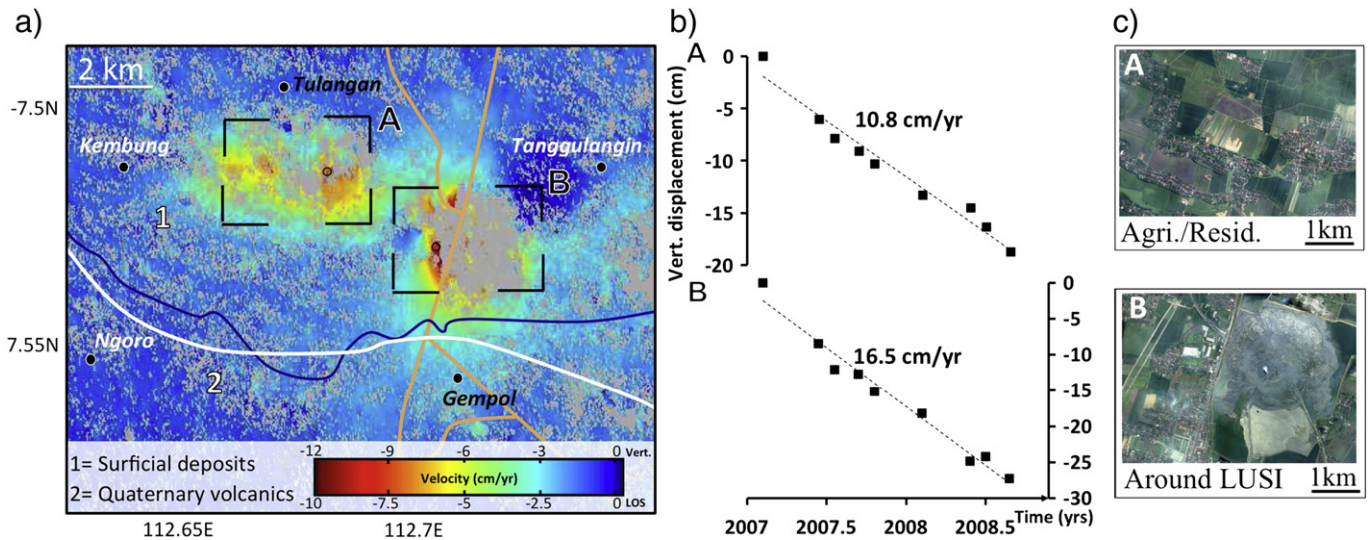


Fig. 11. Same as Fig. 3 for Sidoarjo regency. (For interpretation of the references to color in this figure legend, the reader is referred to the web version of this article.)

Wunut gas field. Gas is extracted from a Pleistocene volcanoclastic reservoir located from 100 to 900 m depth (Kusumastuti et al., 2000). The observed subsidence is likely due to gas extraction from this field.

6.4. Urban areas: large-scale subsidence due to natural and anthropogenic processes

In Medan, Jakarta, Bandung, Blanakan, Pekalongan, and Semarang we observe, in addition to the rapid, patchy subsidence, a large-scale subsidence at rates of 4–6 cm/year (light blue to green colors). These rates are well above the typical subsidence rates associated with natural compaction of Holocene sediments (Table 1, Meckel et al., 2006), suggesting that anthropogenic processes are anyhow involved. The large-scale pattern of the subsidence, its average rates (few cm/year), and its lack of correlation with the land use suggest that it is due to sediment compaction caused by a combination of natural and anthropogenic processes (Table 1). The latter are the effect of past drainage, settlement, and water extraction.

6.5. Subsidence due to other processes

The cause of subsidence at Lusi has been investigated by Fukushima et al. (2009) who concluded that pressure decreases and depletion of material at depth are likely to cause the observed subsidence.

The subsidence observed near Bungbulang is not taking place in compressible deposits but in clastic and volcanic soft rocks (Fig. 10). Groundwater extraction is unlikely responsible for the observed subsidence because of the sharp transitions with the stable surrounding areas and because of the lack of correlation with land use (agricultural and forests). Possible causes of the observed subsidence are solid withdrawal due to mining activities (gem mining is common but no detailed information is available), gas extraction, deforestation and landslides affecting the ground stability, and geothermal activity from the neighboring Cilayu geothermal spring (Herdianita & Priadi, 2008; Hochstein & Sudarman, 2008).

7. Lack of subsidence in other areas

We have identified nine locations experiencing subsidence on the islands of Sumatra, Java, and Bali. It is possible that we missed areas in east Sumatra where no InSAR data are available, and areas subsiding at rates below 2 cm/year. The lack of subsidence in the remaining

major cities of western Indonesia can largely be explained by the absence of compressible deposits. Along the west coast of Sumatra, in western and southern Java, and in southern Bali, surface geology is dominated by limestone, volcanic or metamorphic rocks, which are relatively incompressible. Thus, we do not expect subsidence in cities developed on these sediments. This is consistent with the lack of subsidence in Banda Aceh, Bengkulu, Padang, Bandar Lampung, Serang, Tangerang, Yogyakarta, and Denpasar.

We do not detect subsidence in several cities developed on compressible deposits (Pekanbaru, Depok, Bekasi, and Surabaya). It is possible that subsidence in these cities occurs at rates below our detection threshold of 2 cm/year. The lack of significant subsidence could be because of lower rates of groundwater extraction (limited industrial activities).

8. Consequences and implications of land subsidence

In Indonesia, land subsidence increases the risk of major flooding because many of the subsiding cities and some of the highest subsidence rates are located along the coast at, or near, sea level, and near major rivers.

We estimate the time necessary until the coastal parts of the cities are below relative sea level. In Jakarta, the subsidence rates along the coast vary from 9.5 cm/year to 21.5 cm/year (Fig. 5). Assuming that subsidence continues at an average rate of 10 cm/year and an average elevation above relative sea level of 2 m (SRTM V4 data, Farr et al., 2007) we estimate that the coastal part of Jakarta will be below relative sea level in 20 years. In Lhokseumawe and Medan, with an average elevation of 5 m above relative sea level and a subsidence rate of 8 cm/year, the coastal parts of these cities will be below relative sea level in 60 years. Near Blanakan, Pekalongan and Semarang, with an average elevation taken as 5 m above relative sea level and a subsidence rate of 10 cm/year, the agricultural coastal areas will be below relative sea level in 50 years.

These estimates rely on linear extrapolation of the observed subsidence rates. This, however, may be inaccurate because compaction of aquifers in response to water level decline depends on the physical properties of the aquifer that varies with the stress history (e.g. Terzaghi, 1925). Two processes with opposite effects can affect the time-varying component of the subsidence. Aquifer compaction causes steady land subsidence, but, as the aquifer compaction limit is reached, subsidence is slowing down (e.g. Kim et al., 2010; Terzaghi, 1925). In this case our approximations based on linear extrapolation underestimate the time

Table 2
 Compilation of the observations made in the nine locations experiencing subsidence. AR = average rates of subsidence (light blue to green colors), HR = high rates of subsidence (red to yellow colors). We relate these observations to the characteristics of each process creating subsidence (in Table 1) to isolate the causes of subsidence (last column).

Location	Average LOS rate (cm/year)	Max LOS rate (cm/year)	Av. vert. rate (cm/year)	Max vert. rate (cm/year)	Spatial pattern AR = average rate HR = high rates	Surface geology	Correl. with surface geol.	Land use	Correl. with land use	Interpreted cause of rapid subs.
Lhokseumawe (Fig. 3)	3.5	9.4	4.2	11.3	Local	Surficial deposits	N	Agricult. and resident.	N, but on Arun gas field	Gas extraction
Medan (Fig. 4)	4	6.9	4.8	8.3	AR = large HR = patchy	Surficial and swamp deposits	N	Industrial	Y	Industrial water extraction
Jakarta (Fig. 5)	6	18.2	7.2	21.8	AR = large HR = patchy	Surficial deposits	N	Industrial	Y	Industrial water extraction
Bandung (Fig. 6)	6	18.8	7.2	22.5	AR = large HR = patchy	Surficial deposits	N	Industrial	Y	Industrial water extraction
Blanakan (Fig. 7)	4	10	4.8	12.0	AR = large HR = patchy	Surficial deposits	N	Agricult.	Y	Agricult. water extraction
Pekalongan (Fig. 8)	4	8.8	4.8	10.5	AR = large HR = patchy	Surficial deposits	N	Agricult. and resident.	Y	Agricult. water extraction
Semarang (Fig. 9)	4	10.8	4.8	13.0	AR = large HR = patchy	Surficial deposits	N, but no subs. on limestone	Industrial	Y	Industrial water extraction
Bungbulang (Fig. 10)	5	12.6	6	15.1	Local	Clastic and volcanic deposits	N	Agricult. and forests	N	?
Sidoarjo (Fig. 11)	4	13.8	4.8	16.5	Local	Surficial deposits	N	– East: Lusi – West: agri. and resid.	– East: Y – West: N, Wunut gas field	– East: Lusi eruption – West: Gas extraction

until coastal areas are below relative sea level. However the subsidence rates measured in Jakarta between 2007 and 2009 are similar to the ones measured in 1997, suggesting that subsidence shows no signs of deceleration. Moreover, we need to consider that even after cessation of water extraction, subsidence will still occur due to residual compaction. The combination of these last two observations suggests that linear rates are appropriate to give a general estimate of the time necessary until the coastal parts of the cities are below relative sea level.

Sea level rise is further worsening the situation. Regional sea level is currently increasing at a rate of 1.5–4.4 mm/year (Mimura & Yokoki, 2004), and expected to accelerate 2–3 folds in the next 1–2 decades (IPCC, 2007). Sea level rise shortens the time until coastal areas are below relative sea level by 3–5% (Badshah & Perlman, 1996; Dasgupta et al., 2009).

Finally, the heavy rainfall associated with the monsoon, the storms and tropical cyclones, the lack of coastal or river defenses, as well as the limited evacuation potential, increase the vulnerability of those Indonesian cities. Our estimates emphasize the urgency of hazard mitigation programs to slow down the subsidence processes and reduce the risk of inundation.

9. Conclusion

InSAR time-series provide unprecedented spatial resolution and continuous temporal coverage of the subsidence in western Indonesia. We identified nine locations undergoing subsidence at rates up to 22.5 cm/year. Groundwater extraction for industrial use is responsible for rapid, patchy subsidence in Medan, Jakarta, Bandung, and Semarang, while groundwater extraction for agricultural use is likely responsible for subsidence near Pekalongan and Blanakan. Subsidence due to gas extraction is observed in the Arun and Wunut gas fields, near Lhokseumawe and in the Sidoarjo regency, respectively.

If not addressed, subsidence will lead to an increase of inundation both in frequency and spatial extent, and will put coastal cities below relative sea level within decades. Moreover, because loss of elevation due to aquifer compaction is mostly irreversible, protection of land from flooding requires construction of permanent defenses, but these structures are only temporary unless subsidence is stopped.

Acknowledgments

We thank the National Aeronautics and Space Administration (NASA) and the National Science Foundation (NSF) for the support (NNX09AK72G and EAR-0810214). The ALOS-PALSAR data are copyright of the Japanese Space Agency (JAXA) and the Japanese Ministry of Economy, Trade and Industry (METI) and was made available by the U.S. Government Research Consortium (USGRC) and the Alaska Satellite Facility (ASF).

Appendix A. Supplementary data

Supplementary data to this article can be found online at <http://dx.doi.org/10.1016/j.rse.2012.10.015>.

References

- Abidin, H., Andreas, H., Djaja, R., Darmawan, D., & Gamal, M. (2008). Land subsidence characteristics of Jakarta between 1997 and 2005, as estimated using GPS surveys. *GPS Solutions*, 12(1), 23–32. <http://dx.doi.org/10.1007/s10291-007-0061-0>.
- Abidin, H., Andreas, H., Gamal, M., Djaja, R., Murdohardono, D., Rajiyowiryono, H., et al. (2006). Studying land subsidence of Bandung Basin (Indonesia) using GPS survey technique. *Survey Review*, 38(299), 397–405.
- Abidin, H., Andreas, H., Gumilar, I., Fukuda, Y., Pohan, Y. E., & Deguchi, T. (2011a). Land subsidence of Jakarta (Indonesia) and its relation with urban development. *Natural Hazards*, 59(3), 1753–1771. <http://dx.doi.org/10.1007/s11069-011-9866-9>.
- Abidin, H., Andreas, H., Gumilar, I., Sidiq, T. P., & Fukuda, Y. (2012). Land subsidence in coastal city of Semarang (Indonesia): Characteristics, impacts and causes. *Geomatics, Natural Hazards and Risk*, 1–15. <http://dx.doi.org/10.1080/19475705.2012.692336>.
- Abidin, H., Andreas, H., Gumilar, I., Sidiq, T., Gamal, M., Murdohardono, D., et al. (2010). Studying land subsidence in Semarang (Indonesia) using geodetic methods. *FIG Congress, Facing the Challenges—Building the Capacity*, Sydney, Australia.
- Abidin, H., Djaja, R., Andreas, H., Gamal, M., Hirose, K., & Maruyama, Y. (2004). Capabilities and constraints of geodetic techniques for monitoring land subsidence in the urban areas of Indonesia. *Geomatics Research Australia*, 81, 45–58.
- Abidin, H., Djaja, R., Darmawan, D., Hadi, S., Akbar, A., Rajiyowiryono, H., et al. (2001). Land subsidence of Jakarta (Indonesia) and its geodetic monitoring system. *Natural Hazards*, 23, 365–387.
- Abidin, H., Gumilar, I., Andreas, H., Sidiq, P. T., & Fukuda, Y. (2011b). Study on causes and impacts of land subsidence in Bandung Basin, Indonesia. *FIG Working Week 2011 Bridging the Gap between Cultures Marrakech, Morocco, 18–22 May 2011*.
- Amelung, F., Galloway, D. L., Bell, J., Zebker, H. A., & Laczniak, R. (1999). Sensing the ups and downs of Las Vegas: InSAR reveals structural control of land subsidence and aquifer-system deformation. *Geology*, 27(6), 483–486.
- Badshah, A. A., & Perlman, J. E. (1996). Mega-cities and the urban future. *City*, 1(3–4), 122–132.
- Bell, J., Amelung, F., Ramelli, A., & Blewitt, G. (2002). Land subsidence in Las Vegas, Nevada, 1935–2000: New geodetic data show evolution, revised spatial patterns, and reduced rates. *Environmental and Engineering Geoscience*, 8(3), 155–174.
- Berardino, P., Fornaro, G., Lanari, R., & Sansosti, E. (2002). A new algorithm for surface deformation monitoring based on small baseline differential SAR interferograms. *IEEE Transactions on Geoscience and Remote Sensing*, 40(11), 2375–2383. <http://dx.doi.org/10.1109/TGRS.2002.803792>.
- Bock, Y., Wdowinski, S., Ferretti, A., Novali, F., & Fumagalli, A. (2012). Recent subsidence of the Venice Lagoon from continuous GPS and interferometric synthetic aperture radar. *Geochemistry, Geophysics, Geosystems*, 13, Q03023. <http://dx.doi.org/10.1029/2011GC003976>.
- Braadbaart, O., & Braadbaart, F. (1997). Policing the urban pumping race: Industrial groundwater overexploitation in Indonesia. *World Development*, 25(2), 199–210.
- Burbey, T. (2002). The influence of faults in basin-fill deposits on land subsidence, Las Vegas Valley, Nevada, USA. *Hydrogeology Journal*, 10(5), 525–538. <http://dx.doi.org/10.1007/s10040-002-0215-7>.
- Cabral-Cano, E., Dixon, T. H., Miralles-Wilhelm, F., Diaz-Molina, O., Sanchez-Zamora, O., & Carande, R. E. (2008). Space geodetic imaging of rapid ground subsidence in Mexico City. *Geological Society of America Bulletin*, 120(11–12), 1556–1566. <http://dx.doi.org/10.1130/B26001.1>.
- Chan, F. K. S., Mitchell, G., Adekola, O., & McDonald, A. (2012). Flood risk in Asia's urban mega-deltas: Drivers, impacts and response. *Environment and Urbanization ASIA*, 3(1), 41–61. <http://dx.doi.org/10.1177/097542531200300103>.
- Chaussard, E., & Amelung, F. (in press). Precursory inflation of shallow magma reservoirs at west Sunda volcanoes detected by InSAR. *Geophysical Research Letters*. <http://dx.doi.org/10.1029/2012GL053817>.
- Damoah-Afari, P., Ding, X., Li, Z., Lu, Z., & Omura, M. (2007). Six years of land subsidence in Shanghai revealed by JERS-1 SAR data. *Geoscience and Remote Sensing Symposium*, 2007. IGARSS 2007. IEEE International, 2093–2097.
- Dasgupta, S., Laplante, B., Meisner, C., Wheeler, D., & Yan, J. (2009). The impact of sea level rise on developing countries: A comparative analysis. *Climatic Change*, 93(4), 379–388. <http://dx.doi.org/10.1007/s10584-008-9499-5>.
- Delinon, R. M. (2008). Groundwater management issues in the Greater Jakarta area, Indonesia. *Proceedings of International Workshop on Integrated Watershed Management for Sustainable Water Use in a Humid Tropical Region. JSPS-DGHE 485 Joint Research Project*, 8. (pp. 40–54).
- Dixon, T. H., Amelung, F., Ferretti, A., Novali, F., Rocca, F., Dokka, R., et al. (2006). Space geodesy: Subsidence and flooding in New Orleans. *Nature*, 441(7093), 587–588. <http://dx.doi.org/10.1038/441587a>.
- Farr, T. G., Caro, E., Crippen, R., Duren, R., Hensley, S., Kobrick, M., et al. (2007). The shuttle radar topography mission. *Reviews of Geophysics*, 45, RG2004. <http://dx.doi.org/10.1029/2005RG000183>.
- Fattahi, H., & Amelung, F. (in press). DEM error correction in InSAR time-series. *IEEE Transactions on Geoscience and Remote Sensing*.
- Feng, Q.-Y., Liu, G.-J., Meng, L., Fu, E.-J., Zhang, H., & Zhang, K. (2008). Land subsidence induced by groundwater extraction and building damage level assessment—A case study of Datun, China. *Journal of China University of Mining and Technology*, 18(4), 556–560.
- Fruneau, B., & Sarti, F. (2000). Detection of ground subsidence in the city of Paris using radar interferometry: Isolation of deformation from atmospheric artifacts using correlation. *Geophysical Research Letters*, 27(24), 3981–3984.
- Fukushima, Y., Mori, J., Hashimoto, M., & Kano, Y. (2009). Subsidence associated with the LUSI mud eruption, East Java, investigated by SAR interferometry. *Marine and Petroleum Geology*, 26(9), 1740–1750. <http://dx.doi.org/10.1016/j.marpetgeo.2009.02.001>.
- Gabriel, A., Goldstein, R., & Zebker, H. A. (1989). Mapping small elevation changes over large areas — Differential radar interferometry. *Journal of Geophysical Research—Solid Earth and Planets*, 94, 9183–9191.
- Geological Survey Institute of Indonesia (GRDC) (2008). Geological map of Indonesia. available online at, <http://geologicalmap.esdm.go.id/>
- Guéguen, Y., Deffontaines, B., Fruneau, B., Heib, A., de Michele, M., Raucoules, D., et al. (2009). Monitoring residual mining subsidence of Nord/Pas-de-Calais coal basin from differential and persistent scatterer interferometry (Northern France). *Journal of Applied Geophysics*, 69(1), 24–34. <http://dx.doi.org/10.1016/j.jappgeo.2009.02.008>.
- Hanssen, R. F. (2001). *Radar interferometry: Data interpretation and error analysis*. Dordrecht, The Netherlands: Kluwer Academic Publishers.
- Heleno, S. I. N., Oliveira, L. G. S., Henriques, M. J., Falcão, A. P., Lima, J. N. P., Cooksley, G., et al. (2011). Persistent scatterers interferometry detects and measures ground subsidence in Lisbon. *Remote Sensing of Environment*, 115(8), 2152–2167. <http://dx.doi.org/10.1016/j.rse.2011.04.021>.

- Helm, D. C. (1978). Field verification of a one-dimensional mathematical model for transient compaction and expansion of a confined aquifer system. *Verification of mathematical and physical models in hydraulic engineering. Proceedings 26th Hydraulic Division Specialty Conference* (pp. 189–196).
- Herdianita, N., & Priadi, B. (2008). The chemical compositions of thermal waters at Ciarinem and Cilayu, Pameungpeuk, West Java—Indonesia. *ITB Journal of Science*, 40(1), 49–61.
- Hochstein, M. P., & Sudarman, S. (2008). History of geothermal exploration in Indonesia from 1970 to 2000. *Geothermics*, 37(3), 220–266. <http://dx.doi.org/10.1016/j.geothermics.2008.01.001>.
- Hoffmann, J., Zebker, H. A., & Galloway, D. L. (2001). Seasonal subsidence and rebound in Las Vegas Valley, Nevada, observed by synthetic aperture radar interferometry. *Water Resources Research*, 37(6), 1551–1566.
- IPCC (2007). IPCC: Synthesis report. *Contribution of working groups I – Fourth assessment report of the Intergovernmental Panel on Climate Change*. Cambridge, UK: Cambridge Univ Press.
- Kim, S. -W. W., Wdowinski, S., Dixon, T. H., Amelung, F., Kim, J. W., & Won, J. -S. (2010). Measurements and predictions of subsidence induced by soil consolidation using persistent scatterer InSAR and a hyperbolic model. *Geophysical Research Letters*, 37(5), <http://dx.doi.org/10.1029/2009GL014644>.
- Kuehn, F., Albiol, D., Cooksley, G., Duro, J., Granda, J., Haas, S., et al. (2010). Detection of land subsidence in Semarang, Indonesia, using stable points network (SPN) technique. *Environmental Earth Sciences*, 60(5), 909–921. <http://dx.doi.org/10.1007/s12665-009-0227-x>.
- Kusumastuti, A., Darmoyo, A. B., Suwarlan, W., & Sosromihardjo, S. (2000). *The Wunut field: Pleistocene volcanoclastic gas sands in East Java*.
- Lubis, A. M., Sato, T., Tomiyama, N., Isezaki, N., & Yamanokuchi, T. (2011). Ground subsidence in Semarang—Indonesia investigated by ALOS-PALSAR satellite SAR interferometry. *Journal of Asian Earth Sciences*, 40(5), 1079–1088. <http://dx.doi.org/10.1016/j.jseae.2010.12.001>.
- Massonnet, D., Rossi, M., Carmona, C., Adragna, F., Peltzer, G., Feigl, K. L., et al. (1993). The displacement field of the Landers earthquake mapped by radar interferometry. *Nature*, 364, 138–142.
- Mazzini, A., Svendsen, H., Akhmanov, G. G., Aloisi, M., Planke, S., Malthe-Sørensen, A., et al. (2007). Triggering and dynamic evolution of the LUSI mud volcano, Indonesia. *Earth and Planetary Science Letters*, 261(3–4), 375–388. <http://dx.doi.org/10.1016/j.epsl.2007.07.001>.
- Mazzotti, S., Lambert, A., Van der Kooij, M., & Mainville, A. (2009). Impact of anthropogenic subsidence on relative sea-level rise in the Fraser River delta. *Geology*, 37(9), 771–774. <http://dx.doi.org/10.1130/G25640A.1>.
- Meckel, T. A. (2008). An attempt to reconcile subsidence rates determined from various techniques in southern Louisiana. *Quaternary Science Reviews*, 27(15–16), 1517–1522. <http://dx.doi.org/10.1016/j.quascirev.2008.04.013>.
- Meckel, T. A., Brink, ten, U. S., & Williams, S. J. (2006). Current subsidence rates due to compaction of Holocene sediments in southern Louisiana. *Geophysical Research Letters*, 33(11), <http://dx.doi.org/10.1029/2006GL026300>.
- Mimura, N., & Yokoki, H. (2004). Sea level changes and vulnerability of the coastal region of East Asia in response to global warming. *SCOPE/START monsoon Asia rapid assessment report*.
- Osmanoglu, B., Dixon, T. H., Wdowinski, S., Cabral-Cano, E., & Jiang, Y. (2011). Mexico City subsidence observed with persistent scatterer InSAR. *International Journal of Applied Earth Observations and Geoinformation*, 13(1), 1–12. <http://dx.doi.org/10.1016/j.jag.2010.05.009>.
- Raucoules, D., Colesanti, C., & Carnec, C. (2007). Use of SAR interferometry for detecting and assessing ground subsidence. *Comptes Rendus Geosciences*, 339(5), 289–302. <http://dx.doi.org/10.1016/j.crte.2007.02.002>.
- Rosen, P. A., Hensley, S., Peltzer, G., & Simons, M. (2004). Updated repeat orbit interferometry package released. *Eos, Transactions American Geophysical Union*, 85(5), <http://dx.doi.org/10.1029/2004EO050004> 47–.
- Schmidt, G., Soefner, B., & Soekardi, P. (1990). Possibilities for groundwater development for the city of Jakarta, Indonesia. *IAHS Publication, Int. Assoc. of Hydrological Sciences, Wallingford (Engl)*, 198. (pp. 233–242).
- Sestini, G. (1996). Land subsidence and sea-level rise: the case of the Po Delta region, Italy. In J. D. Milliman, & B. U. Haq (Eds.), *Sea-level rise and coastal subsidence* (pp. 235–248). : Kluwer Academic Publishers.
- Soeparjadi, R. A. (1983). Geology of the Arun gas field. *Journal of Petroleum Technology*, 35(6), <http://dx.doi.org/10.2118/10486-PA>.
- Soetrisno, S. (1996). Impacts of urban and industrial development on groundwater, Bandung, West Java, Indonesia. *Symposium on groundwater and landuse planning, Fremantle, Western Australia, 16–18 September 1996*.
- Teatini, P., Tosi, L., & Strozzi, T. (2011). Quantitative evidence that compaction of Holocene sediments drives the present land subsidence of the Po Delta, Italy. *Journal of Geophysical Research*, 116(B8), <http://dx.doi.org/10.1029/2010JB008122>.
- Terzaghi, K. (1925). *Erdbaumechanik (introduction to soil mechanics)* (pp. 1943–1944). Vienna: Franz Deuticke.
- Tesauro, M., Berardino, P., Lanari, R., Sansosti, E., Fornaro, G., & Franceschetti, G. (2000). Urban subsidence inside the city of Napoli (Italy) observed by satellite radar interferometry. *Geophysical Research Letters*, 27(13), 1961–1964.
- Tizzani, P., Berardino, P., Casu, F., Euillades, P., Manzo, M., Ricciardi, G. P., et al. (2007). Surface deformation of Long Valley caldera and Mono Basin, California, investigated with the SBAS-InSAR approach. *Remote Sensing of Environment*, 108(3), 277–289. <http://dx.doi.org/10.1016/j.rse.2006.11.015>.
- Törnqvist, T. E., Wallace, D. J., Storms, J. E. A., Wallinga, J., van Dam, R. L., Blauw, M., et al. (2008). Mississippi delta subsidence primarily caused by compaction of Holocene strata. *Nature Geoscience*, 1(3), 173–176. <http://dx.doi.org/10.1038/ngeo129>.
- Wright, T. J., Parsons, B. E., & Lu, Z. (2004). Toward mapping surface deformation in three dimensions using InSAR. *Geophysical Research Letters*, 31(1), L01607. <http://dx.doi.org/10.1029/2003GL018827>.
- Yan, X. X., & Gong, S. L. (2002). Relationship between building density and land subsidence in Shanghai urban zone (in Chinese). *Hydrogeology and Engineering Geology*, 29(6), 21–25.
- Yuill, B., Lavoie, D., & Reed, D. (2009). Understanding subsidence processes in coastal Louisiana. *Journal of Coastal Research*, 23–36.